Int. J. Electrochem. Sci., 7 **(2012)** 10132 - 10141

International Journal of
ELECTROCHEMICAL
SCIENCE
www.electrochemsci.org

Polymers Nucleation and Growth Mechanism: Solubility, a Determining Factor

M. Romero, M. A. del Valle[*]*, R. del Río, F. R. Díaz, F. Armijo*

Pontificia Universidad Católica de Chile, Facultad de Química, Departamento de Química Inorgánica, Laboratorio de Electroquímica de Polímeros (LEP), Vicuña Mackenna 4860, 7820436, Macul, Santiago, Chile.
[*]E-mail: mdvalle@uc.cl

Received: 28 August 2012 / *Accepted:* 18 September 2012 / *Published:* 1 October 2012

Temperature and ultrasound effect on the nucleation and growth mechanisms (NGM) of *poly(ortho-toluidine)* (POT) was investigated. Synthesis conditions at temperatures between 263 and 303 K were optimized with and without ultrasonic irradiation. The obtained i-t transient is complex and its deconvolution showed to be made up of three contributions that initially included a progressive nucleation with bidimensional growth (PN2D), along with two progressive nucleation contributions with three-dimensional growth, one controlled by diffusion and the other by charge transfer, PN3Ddif and PN3Dct, respectively. Besides, as temperature decreases, a decrease of the charge associated to each contribution was observed. At the same time the nucleation induction time increases, as occurs when ultrasound is applied during the electro-polymerization. This effect was ascribed to kinetic factors rather than to film conductivity. Conductivity measurements of deposits obtained at different temperature corroborated this issue. *In situ* spectro-electrochemical studies were accomplished to analyze differences between polymer films obtained by varying the temperature. The results enabled the proposed electro-polymerization model to be validated: it was found that the electro-deposition process initially depends on oligomers solubility at the electrode-solution interface. When these oligomers reach a chain length at which are insoluble, they precipitate on the electrode surface, giving rise to the nuclei that establish the onset of the polymer electro-deposition process. Also, these results explain the important effect of temperature and ultrasound on the NGM, because these variables directly affect solubility, a determining factor in electro-polymerization.

Keywords: Keywords: *o*-toluidine**,** poly(*o*-toluidine), electro-polymerization, nucleation and growth mechanism, conducting polymers.

1. INTRODUCTION

Although during the last decades the electrochemical synthesis of conducting polymers on metallic substrates has been thoroughly studied [1-8], a contribution to understanding polymers

formation mechanism remains a necessity. In this context, our group has carried out a variety of studies on the electro-deposition of conducting polymers, systematically analyzing the effect of experimental variables that govern the process (starting unit, solvent, monomer type and concentration, supporting electrolyte concentration and type, electro-polymerization applied potential) [9-12], that enabled an electro-polymerization mechanism model to be put forward, Scheme 1 [13].

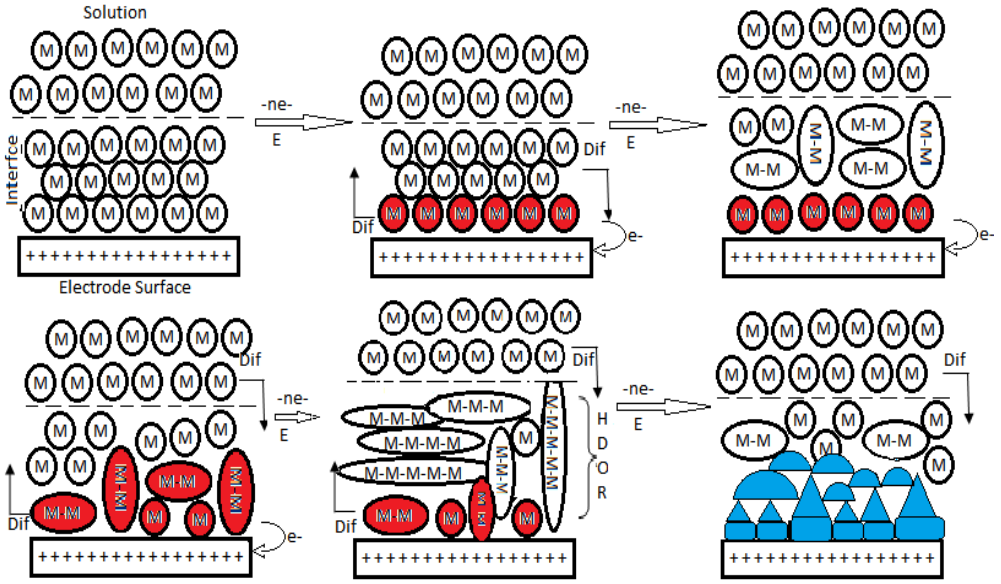

Scheme1. Schematic representation of the model proposed for the NG process in the electro-polymerization: M = monomer, ○ neutral species, ● = radical cations ("oxidized species"), and ▲ ▬ ⌓ oligomeric clusters.

Furthermore, studies exist regarding temperature effect on PANI morphology during its electro-polymerization. It was verified that at low temperature, electro-synthesized PANI presented high conductivity and lower molecular weight, ascribed to intra-chain conductivity in the polymer film [14]. Other authors have investigated poly(*o*-anisidine), POAN, electro-polymerization [15] and found a better POAN growth when electro-synthesized at 288 K using a potentiodynamic method. It is noteworthy that all syntheses conducted by these authors were performed within the same potential window for each working temperature. Other authors analyzed the effect of ultrasonic radiation on PEDOT electro-polymerization. They found this perturbation improved doping properties of the polymeric film owing to an increase of mass transfer coefficient that is intrinsically related to the diffusion coefficient [16]. However, no record exists about a systematic study regarding temperature and ultrasound effect on the NGM during the electro-preparation of polymer films on metal substrates. NGMs provide information at molecular level of how the polymeric film is generated on the electrode surface, enabling thus synthesis strategies to be developed for obtaining polymer coatings with the desired properties. Consequently, a systematic study is suggested here to corroborate the electro-polymerization model and explain, from that point of view, the described results. As summarized in Scheme 1, the proposed NGM model for the electro-deposition of conducting polymers establishes that

the polymer nucleation process (and subsequent growth) at the electrode surface depends on the degree of saturation of the high density oligomeric region, HDOR, *i.e.* is determined by the solubility of the oligomers present at the electrode-solution interface. In other words, when the growing oligomer reaches a critical chain length at the interface that makes it insoluble in the electrolytic solution, precipitation upon the electrode surface occurs, originating nuclei that cause polymer film growth. Therefore, to go deeper into the verification of this model, a systematic analysis of the effect of two important parameters that affect the solubility, namely temperature and ultrasound, is proposed. The goal of the current work was to ascertain whether precipitation of oligomers, whose length make them insoluble, is indeed the variable that determines the formation of different nuclei that bring about the polymeric deposit growth, determining thus film morphology and macroscopic properties, *e.g.* conductivity or doping.

2. EXPERIMENTAL

A 0.07 cm^2 geometric area polycrystalline platinum disk and a Pt coil of large surface area were used as working and counter electrode, respectively. Ag|AgCl in tetramethylammonium chloride, whose potential matches that of a saturated calomel electrode at room temperature, was used as reference electrode [17]. Unless otherwise stated all potential quoted in this work are referred to this electrode.

2 $mol \cdot L^{-1}$ H_2SO_4 (Merck) in ultrapure water (18.2 $M\Omega \cdot cm$ resistivity) was the supporting electrolyte. 0.5 $mol \cdot L^{-1}$ *o*-toluidine (Aldrich, 99.5% purity) was prepared in the supporting electrolyte. Prior to each experiment the solution was deaerated by purging with high purity argon. The optimum polymerization conditions (monomer and H_2SO_4 concentration and potential window) were determined by cyclic voltammetry (CV). From these results the applied potentiostatic perturbation to obtain i-t transients was selected.

Electrochemical measurements were conducted on a Voltalab PGP201 potentiostat. Temperature was regulated using a bath controlled by a HAAKE G thermostat-cryostat that enables an ethylene glycol-water mixture to flow through the electrochemical cell jacket.

Spectro-electrochemical studies were accomplished on an Analytikjena SPECORD 40 spectrophotometer coupled to Fibre-optical Systems Hellman. The working electrode used in this experiment was a 0.50 cm^2 geometric area Pt grid. The polymerization potential was applied and, simultaneously, 5 sweeps between 280 and 1000 nm were run and the UV-Vis spectra recorded after 30, 60, 90, 120 and 150 s of electro-polymerization. Reference and counter electrodes were those described above.

Electro-synthesized polymer films conductivity was measured by the four-point probing method on a conductometer Jandel system, model RM3-AR.

3. RESULTS AND DISCUSSION

3.1. Cyclic voltammetry

Figure 1 depicts voltammetric profiles obtained during POT electro-polymerization at two extreme working temperatures, 268 and 303 K. Two redox processes were observed corresponding to the transition between the characteristic oxidation states of the aniline derivatives leucoemeraldine-emeraldine and emeraldine-pernigraniline [18]. The first cycle shows that the higher the temperature the lower the polymerization onset potential (0.71 V). At lower temperature this phenomenon starts at 0.74 V. Thus, when studying nucleation and growth processes a greater potential should be applied as temperature decreases. This implies that at lower temperature more energy will be required to achieve monomer oxidation, and this is reflected in the need to apply a higher oxidation potential.

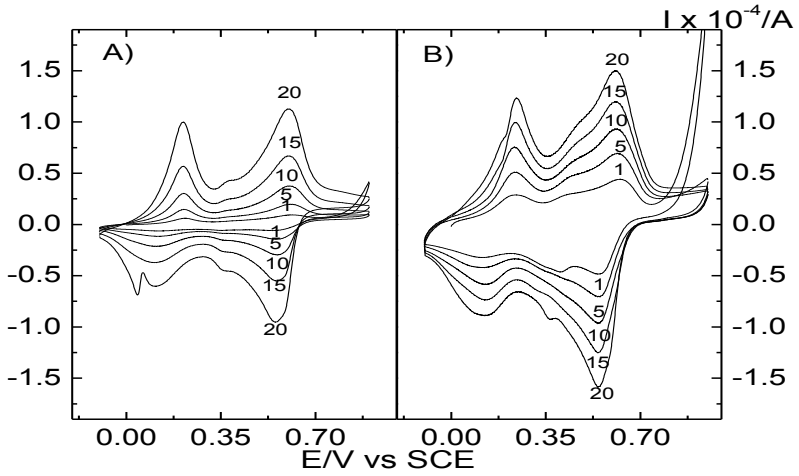

Figure 1. Potentiodynamic profiles for the interface Pt|0.5 mol·L^{-1} OT + 2 mol·L^{-1} H_2SO_4: (A) 303 K, and (B) 268 K. v = 100 mV·s^{-1}.

3.2. Nucleation and growth mechanisms, NGM

To study the NGM, current-time transients at different temperatures were recorded. The first outstanding fact is the induction time (τ) increase with temperature decrease. τ is the time required to exceed oligomers saturation level at the electrode-solution interface, *i.e.* describes the HDOR formation [9-13]. The values in Table 1 can be understood if a polymerization rate decrease is considered, as demonstrated by the lower polymer growth observed in Figure 1.

To obtain NGMs current-time transients, simulation was carried out considering the different contributions to the global NGM that may take place, from the τ value. As seen in Figure 2, it is noteworthy that at all the studied temperatures, transients are complex and, therefore, made up of more than one type of contribution (types of nucleation and subsequent growth), a fact also observed for other polymers, as reported elsewhere [9-13]. Figure 2A shows the dependence of time-current transients on temperature, verifying that as the latter decreases, so does the current. This implies that film electro-deposition occurs to a lesser extent, a phenomenon similar to that observed in Figure 1,

where the current in the profile obtained by CV at 268 K is one order of magnitude lower than at 303 K, demonstrating that temperature has a very marked effect on electro-polymerization kinetics.

Table 1. Induction time (τ) at the studied temperatures

Temperature / K	τ / s
268	63.5
273	49.5
278	44.0
283	34.9
288	30.9
293	27.0
298	24.8
303	23.4

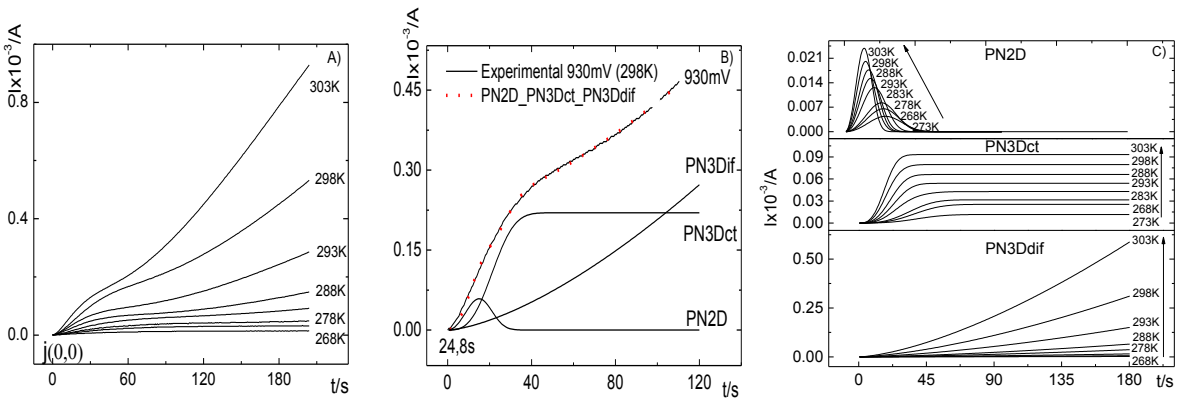

Figure 2. A) Temperature effect on current-time transients obtained in POT electro-synthesis. **B)** Time-current transient deconvolution at 298 K. **C)** Temperature effect on POT NGM contributions. Interface: Pt|0.5 mol·L^{-1} OT + 2 mol·L^{-1} H_2SO_4.

To ascertain whether the current increase in the recorded voltammetric profiles and in the i-t transients in POT electro-synthesis at high temperature could be ascribed to a concomitant conductivity increase of the polymeric film, conductivity of the electro-synthesized polymer was determined at the extreme working temperatures (268 and 303 K). The obtained values are included in Table 2, in which it is seen that the polymer synthesized at the lowest temperature (268 K) presents a slightly lower conductivity than that synthesized at the highest one (303 K). Consequently, the observed current increase in the voltammetric profile and i-t transients during the electro-synthesis can be attributed to kinetic factors that are affected by temperature variation, *e.g.* rate constant of each involved processes, and not to conductivity influence since this property increase is marginal as to be responsible for current increase. However, the slight conductivity increase found at the lowest temperature will be explained later.

Table 2. POT conductivity electro-synthesized at 260 and 303 K.

Temperature / K	Conductivity / 10^{-3} S·cm^{-1}
268	1.92
303	5.97

Figure 2B shows experimental and simulated curves fitting. The simulation is made up of three contributions. At shorter times (less than 15 s), progressive nucleation with bidimensional growth (PN2D) prevails. Subsequently at times between 15 and 30 s, two contributions develop with progressive nucleation and three-dimensional growth predominance, namely one controlled by charge-transfer (PN3Dct) and, at longer times, diffusion controlled (PN3Ddif). It is noteworthy that for all studied temperatures, the mechanism is the same and only induction time increase and total transients charge decrease was observed.

Figure 2C depicts temperature effect on each of the contributions that comprise the overall nucleation and growth mechanism. The plot shows that as temperature decreases, the contributions proportionally decrease and they take longer to get defined. This reveals the temperature is not a variable that modifies the NGM, but only influences current and induction time, *i.e.* changes the process rate but does not alter the mechanism by which the nuclei are generated and grow.

This complex mechanism, made up of different contributions, can be interpreted by considering the previously proposed electro-polymerization model (Scheme 1) [13], *i.e.* the presence of a high density oligomeric region (HDOR). At the beginning of monomer oxidation a high concentration of oxidized monomers are generated at the interface. This provokes the onset of different oligomers formation that once they reach a length at which they become insoluble at the interface, precipitate following a PN2D process. Once the first polymer layer is formed on the electrode, more oligomers precipitate. This further precipitation depends on the oxidized monomer and oligomers being oxidized at the same potential (PN3Dct process). At longer times, monomer diffusion from the bulk of the solution should be expected and, therefore, precipitation following a PN3Ddiff mechanism will commence. Starting from this monomer, nuclei formation was always progressive, *i.e.* different oligomers are obtained that are formed, precipitated and grown at different times. As temperature may affect monomer solubility, Figure 1, it have a pronounced effect on the reaction kinetics, and hence on oligomer formation rate. Thus, i-t transients and each contribution that make them up are developed at shorter times and their charge increases with increasing temperature, validating the proposed model.

Besides, Figure 2C clearly illustrates that temperature exert a greater effect on $PN3D_{dif}$ contribution, due to two reasons. One is the increase of nucleation and growth rate with increasing temperature and the other, diffusion coefficient increase. Consequently, its increase with temperature is more significant than for the other contributions that are affected only by kinetic phenomena.

As for POT NGM, the increase in conductivity at 268 K can be explained as follows. As aforementioned, the NG process at low temperature is slower, delaying the definition of each contribution, indicating that at shorter times bidimensional nucleation-growth predominates affording a

more compact and ordered polymeric film, conferring thus higher conductivity to the electro-synthesized polymer.

3.3. Ultrasound effect

To study ultrasound effect on the electro-polymerization, the same abovementioned experimental conditions and constant temperature (298 K) was utilized. NGM was determined as above, but in this case a 40 kHz ultrasonic perturbation was also employed during the potentiostatic electro-polymerization approach. Figure 3A shows transients obtained in the presence and absence of ultrasound. It can be seen that τ reaches higher values. This suggests that when ultrasound is applied, precipitation on the electrode surface takes much longer and at the same time, the obtained current is much lower than in the absence of this radiation. This can be understood by assuming that ultrasound affects oligomes solubility in the HDOR, increasing it, and therefore it takes longer to reach saturation and subsequent oligomer nuclei deposition.

The nucleation mechanism still remains complex, but not affected by ultrasound, being made up by the same three contributions present in the absence of this disturbance, as observed in the time-current transient deconvolution shown in Figure 3B. This revealed that ultrasound irradiation had no effect on the nucleation mechanism of the polymeric phase. Figure 3C shows a comparison with the transient in the absence of ultrasound. It was observed that, for all contributions, the overall effect implies that the time each contribution takes to develop increases, while the related charge decreases.

Again, this is consistent with the proposed electro-polymerization model because the ultrasound effect is to increase oligomer solubility and, consequently, to decrease the degree of saturation they present in the region close to the electrode, *i.e*. the HDOR.

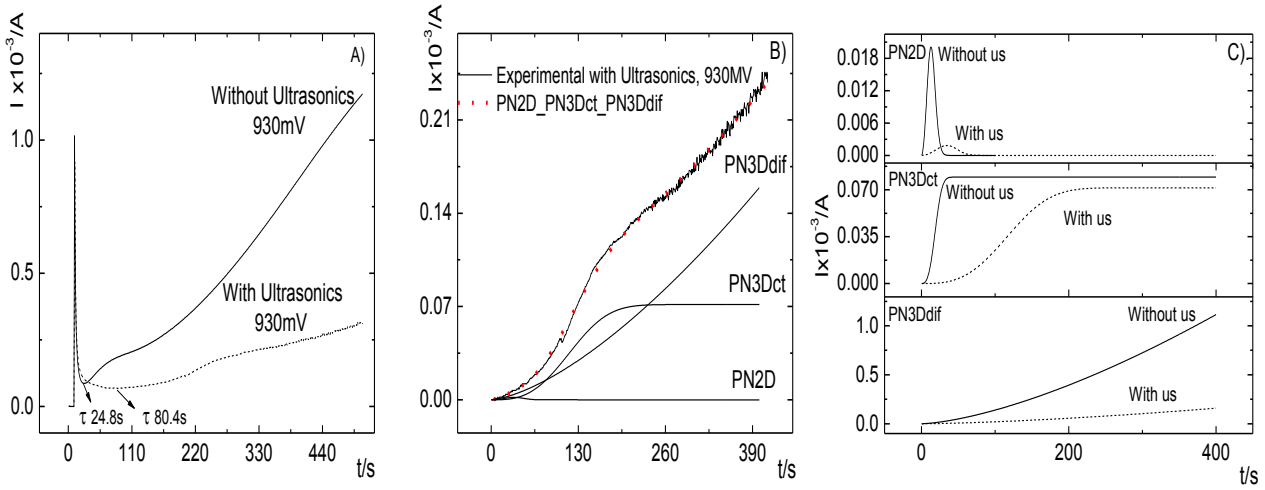

Figure 3. A) Ultrasound effect on POT NGM. Interface: Pt|0.5 mol·L^{-1} OT + 2 mol·L^{-1} H_2SO_4. **B)** Corrected current-time transients deconvolution obtained under ultrasonic irradiation. **C)** NGM comparative study with and without using ultrasound irradiation at 298 K.

3.4. In situ UV-Vis spectro-electrochemistry

In situ spectro-electrochemical studies were conducted utilizing the same abovementioned synthesis conditions in order to compare the signals obtained from successive spectra during the experiment at 268 and 303 K. Figure 4 shows UV-Vis spectra at both temperatures. Only cycles 2, 3 and 4 are shown since cycle 1 displayed just the 272 nm monomer signal. It is worth mentioning that in both spectra three bands, characteristic of doped aniline derivatives [19], at 275, 400 and 715 nm were obtained. Table 3 summarizes the found UV-Vis signals.

The signal at around 280 nm is characteristic of the π-π transition of the benzenoid rings present in both the monomer and the oligomeric species formed from aniline derivatives [18-31]. In this case the signal appeared at 276 nm (4.40 eV) and 286 nm (4.35 eV) for 268 and 303 K respectively, showing a 10 nm hypsochromic shift ascribed to conjugation increase of the oligomers formed in the HDOR [12].

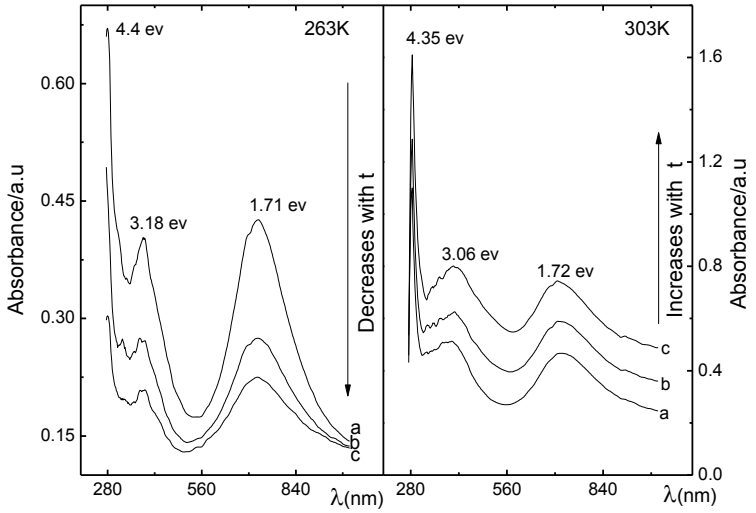

Figure 4. UV-Vis spectra during the electro-polymerization of POT by potentiostatic method under the same synthesis conditions mentioned above. Interface: Pt|0.5 mol·L^{-1} OT + 2 mol·L^{-1} H_2SO_4. a) 30 s, b) 60 s, c) 90 s of electro-synthesis.

Table 3. UV-Vis absorption bands found for OT electro-polymerization at 268 and 303 K.

Temperature / K	λmax1 / nm	λmax2 / nm	λmax3 / nm
268	276	385	730
303	285	412	715

Aromatic radical cations of aniline derivatives displayed a characteristic absorption band at 400 nm (3.10 eV) in aqueous solution. At the lowest temperature used (268 K) this band, as well as the other signals, decreases indicating that the generated species are consumed during electro-polymerization [31]. This is evidenced by a band decrease as the experiment proceeds at this

temperature. In contrast, at high temperature (303 K) this signal increases as the experiment proceeds, implying that at this temperature oligomers are still being produced during the electro-synthesis. With increasing temperature, this band undergoes a 27 nm hypsochromic shift.

Finally, the band at 715 nm (1.72 eV) is assigned to π-π^* transition of quinoid rings present in the POT structure. This signal is characteristic of the emeraldine oxidation state of aniline derived polymers.

Note that at the lowest temperature (268 K) the UV-Vis spectra signal intensities decrease and tend to disappear as the electro-polymerization takes place. This is an indication that the species generated by applying the polymerization potential are consumed as electro-polymerization proceeds. In contrast, at the highest temperature (303 K), it is clearly seen that these absorption bands increase as the electro-polymerization proceeds, revealing that species are being generated during the whole synthetic process.

Bands between 270 and 400 nm at 303 K, are shifted to higher wavelengths, confirming an increase of conjugation due to longer chain oligomers that saturate the HDOR and precipitate on the electrode surface.

All these results demonstrate the validity of the proposed model, because precipitation onto the electrode of oligomers with different chain length, once they meet or exceed the length that makes them insoluble ("critical length"), would be the manner through which nuclei, that give rise to polymeric deposit growth, are formed.

4. CONCLUSIONS

The CV profiles demonstrated that at high temperature a greater amount of polymer film is produced. Furthermore, a lower oxidation potential is required to generate a good electro-polymerization profile.

Current-time transients revealed that a temperature decrease caused an induction time increase, suggesting that at these low temperatures the process is much slower and takes longer to precipitate the oligomers that produce the first nuclei growth. A systematic study on temperature effect enabled verifying that this parameter does not change conducting polymers NGM, it only accelerates the process (different times) and affects the relative amount of the contributions that comprise the overall process. Besides, as temperature increases the charge associated to each contribution increases too and $PN3D_{dif}$ contribution was the most favored one (obviously, temperature mostly affects the diffusion than any of the other phenomena involved).

The polymer coating obtained at 268 K is slightly more conductive than at 303 K, because at low temperature a more compact and homogeneous, *i.e*. more conductive polymer, is obtained.

On the other hand, ultrasonic irradiation caused the induction time to noticeable increase due to oligomers solubility being affected. Longer chain oligomers are thus required to saturate the HDOR and precipitate upon the electrode surface. Finally, *in situ* spectro-electrochemistry allowed the conjugation increase of the aromatic rings of species present at the interface to be corroborated and, definitely, to substantiate the electro-polymerization model proposed herein.

ACKNOWLEDGMENTS
Financial support through Fondecyt Project 1100055 is kindly acknowledged. M. R. thanks CONICYT Doctoral Scholarship 2009, folio: 57090050.

References

1. M. Skompska, M. J. Chmielewski, A. Tarajko, *Electrochem. Comm.,* 9 (2007) 540.
2. P. Wagner, P. H. Aubert, L. Lutsen, D. Vanderzande, *Electrochem. Comm.,* 4 (2002) 912.
3. S. Tirkeş, A. M. Önal, *J. Appl. Electrochem.,* 48 (2010) 865.
4. D. Kowalski, M. Ueda, T. Ohtsuka, *Corr. Sci.,* 50 (2008) 286.
5. N. Zhu, Z. Chang, P. He, Y. Fang, *Electrochim. Acta,* 51 (2006) 3758.
6. A. A. Shah, S. Bilal, R. Holze, *Synth. Met.,* 162 (2012) 356.
7. S. Bilal, R. Holze, *J. Electroanal. Chem.,* 592 (2006) 1.
8. E. Hur, G. Bereket, Y. Sahin, *Curr. Appl. Phys.,* 7 (2007) 597.
9. M. A. del Valle, M. A. Gacitúa, L. I. Canales, F. R. Díaz, *J. Chil. Chem. Soc.,* 3 (2009) 54.
10. R. Schrebler, P. Grez, P. Cury, C. See, M. Merino, H. Gómez, R. Córdova, M. A. del Valle, *J. Electroanal. Chem.,* 430 (1997) 77.
11. M. A. del Valle , P. Cury, R. Schrebler, *Electrochim. Acta,* 48 (2002) 397.
12. M. A. del Valle, M. A. Gacitúa, E. Borrego, P. P. Zamora, F. R. Díaz, M. B. Camarada, M. P. Antilén, J. P. Soto, *Int. J. Electrochem. Sci.,* 7 (2012) 2552.
13. M. A. del Valle, F. R. Díaz, M. E. Bodini, G. Alfonso, G. M. Soto, E. Borrego, *Polym. Int.,* 54 (2005) 526.
14. K. Teshima, K. Yamada, N. Kobayashi, R. Hirohashi, *J. Electroanal. Chem.*, 426 (1997) 97.
15. S. Patil, J. R. Mahajan, M. A. More, P. P. Patil, S. W. Gosavi, S. A. Gangal, *Polym. Int.*, 46 (1998) 99.
16. A. E. Taouil, F. Lallemand, J. Y. Hihn, J. M. Melot, V. Blondeau-Patissier, B. Lakard, *Ultrason. Sonochem.,* 18 (2011) 140.
17. G. A. East, M. A. del Valle, *J. Chem. Educ.* 77 (2000) 97.
18. H. Yang, A. Bard, *J. Electroanal.Chem.,* 339 (1992) 423.
19. D. Kumar, *Synth. Met.,* 114 (2000) 369.
20. S. Yalcinkaya, N. Çolak, *Des. Monomers Polym.,* 15 (2012) 147.
21. M. R. Nabid, Z. Zamiraei, R. Sedghi, *Iran. Polym. J.,* 19 (2010) 9.
22. M. V. Kulkarni, A. K. Viswanath, P. K. Khanna, *Int. J. Polym. Mater.,* 55 (2006) 501.
23. D. D. Borole, U. R. Kapadi, P. P. Mahulikar, D. G. Hundiwale, *Des. Monomers Polym.,* 7 (2004) 45.
24. G. Venugopal, X. Quan, G. E. Johnson, F. M. Houlihan, E. Chin, O. Nalamasu, *Chem. Mater.*, 7 (1995) 271.
25. L. Zhang, B. Hou, Q. Lang, *Am. J. Anal. Chem.,* 2 (2011) 182.
26. O. P. Dmitriev, *J. Colloid Interface Sci.,* 235 (2001) 380.
27. T. Wen, C. Sivakumar, A. Gopalan, *Electrochim. Acta,* 46 (2001) 1071.
28. J. E. Albuquerque, L. H. C. Mattoso, D. T. Balogh, R. M. Faria, J. G. Masters, A. MacDiarmid, *Synth. Met.,* 113 (2009) 19.
29. O. P. Dmitriev, *Synth. Met.,* 122 (2001) 315.
30. A. P. Monkman, D. Bloor, G. C. Stevens, J. C. H. Stevens, *J. Phys. D: Appl. Phys.,* 20 (1987) 1337.
31. D. Wei, C. Kvarnström, T. Lindfors, L. Kronberg, R. Sjöholm, A. Ivaska, *Synth. Met.,* 156 (2006) 541.